AIP Journal of Applied Physics

Calculation of x-ray intensity from a rough sample based on a statistical model

Bing Hwang and C. R. Houska

Citation: Journal of Applied Physics **63**, 5346 (1988); doi: 10.1063/1.340350
View online: http://dx.doi.org/10.1063/1.340350
View Table of Contents: http://scitation.aip.org/content/aip/journal/jap/63/11?ver=pdfcov
Published by the AIP Publishing

Articles you may be interested in

Sample-morphology effects on x-ray photoelectron peak intensities
J. Vac. Sci. Technol. A **31**, 021402 (2013); 10.1116/1.4774214

Statistical cumulant average theory for describing the grazing-incidence small-angle X-ray scattering from rough surfaces
AIP Conf. Proc. **1476**, 105 (2012); 10.1063/1.4751575

Statistical shape model-based reconstruction of a scaled, patient-specific surface model of the pelvis from a single standard AP x-ray radiograph
Med. Phys. **37**, 1424 (2010); 10.1118/1.3327453

Measurement and Calculation of Absolute X-Ray Intensities
J. Appl. Phys. **42**, 4044 (1971); 10.1063/1.1659722

Calculation of X-Ray Intensities from Electron Probe Specimens
J. Appl. Phys. **32**, 387 (1961); 10.1063/1.1736015

MIT LINCOLN LABORATORY CAREERS

Discover the satisfaction of innovation and service to the nation

- Space Control
- Air & Missile Defense
- Communications Systems & Cyber Security
- Intelligence, Surveillance and Reconnaissance Systems
- Advanced Electronics
- Tactical Systems
- Homeland Protection
- Air Traffic Control

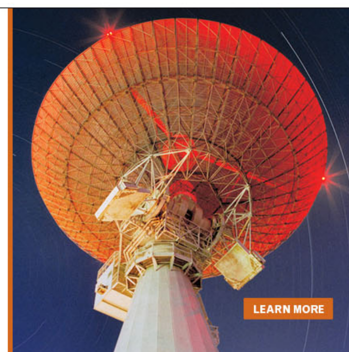

[This article is copyrighted as indicated in the article. Reuse of AIP content is subject to the terms at: http://scitation.aip.org/termsconditions. Downloaded to] IP: 128.173.126.47 On: Wed, 06 May 2015 20:20:25

Calculation of x-ray intensity from a rough sample based on a statistical model

Bing Hwang and C. R. Houska
Department of Materials Engineering, Virginia Polytechnic Institute and State University, Blacksburg, Virginia 24061

(Received 21 October 1987; accepted for publication 28 January 1988)

An x-ray intensity correction is developed which begins with a roughness model that is often used to describe real surfaces. This is based upon a normal distribution of surface asperities relative to a mean plane. Pair correlation between absorbing elements along x-ray paths either entering or leaving the sample with respect to the signal producing element is accomplished by means of an exponential autocorrelation function. This allows the degree of roughness to be varied on a local scale to fit specific surfaces using statistical data. Equations are developed to describe x-ray fluorescence and diffraction signals for symmetric and asymmetric beam optics. Theory is compared with experiment using a roughened, fully stabilized zirconia sample.

INTRODUCTION

A correction by Harrison and Paskin[1] deals with the effect of granularity on the diffracted x-ray intensity from powders. The absorption lengths associated with a signal-producing element in powders is changed from the ideal value for a theoretically dense sample to a smaller value due to the presence of pores. Partial correlations of the absorption lengths for the incident and scattered rays produce an intensity correction relative to a theoretically dense sample. Likewise, for a rough sample, the absorption lengths for pairs of incident and scattered rays are altered by surface roughness and the intensity falls below that of an ideally flat sample. Granularity and roughness effects are similar in the sense that both produce a distribution of path lengths at each fixed depth below the sample surface. Harrison and Paskin's work is restricted to symmetrical x-ray optics, i.e., the incident and scattered rays must make the same angle with the mean sample surface. Also, it is not easily applied to surfaces described by statistical functions.

An exact calculation for a 45° sawtooth surface was made by Borie.[2] Although such a surface differs greatly from reality, this calculation has the value in providing physical insight to the roughness problem and in establishing an upper limit for the correction over a full range of scattering angles. As one might expect, the maximum correction occurs when both rays are parallel to the sawtooth making an angle of 45° with the mean surface. Again, symmetrical x-ray optics as well as a common absorption coefficient for incident-signal pairs were assumed.

This work makes use of a generally accepted statistical model to describe surface asperities,[3] and thereby represents a first treatment for the roughness effect from real surfaces. We assume that the heights of the surface profile are normally distributed with a standard deviation σ, and the pair correlation between different asperities is determined by an autocorrelation function which decays exponentially with distance. This latter parameter controls the degree of roughness on a local scale. The restrictions of symmetrical optics and a common absorption coefficient for the incident and the signal rays are avoided. The latter allows a treatment of x-ray fluorescence as well as diffraction problems for a range of optical paths. Data are presented for a severely ground zirconia sample that are in agreement with the statistical model developed herein.

THE STATISTICAL ROUGHNESS MODEL—ABSORPTION

We use a normal distribution function to describe the heights of surface excursions:

$$p(Z_s) = (1/\sqrt{2\pi\sigma})e^{-Z_s^2}, \qquad (1)$$

where σ is the standard deviation and Z_s is the height measured from the mean surface scaled in units of $\sqrt{2\sigma}$. A pair of excursion heights at two positions separated by a horizontal distance τ are distributed according to the following two-dimensional normal distribution function:

$$p(Z_{1s},Z_{2s},\tau) = \frac{1}{2\pi\sigma^2\sqrt{1-\rho(\tau)^2}} \times e^{-\{[Z_{1s}^2 - 2\rho Z_{1s}Z_{2s} + Z_{2s}^2]/(1-\rho(\tau)^2)\}}, \qquad (2)$$

where Z_{1s} and Z_{2s} are the scaled heights at two positions and $\rho(\tau)$ is the autocorrelation coefficient function which determines the degree of likeness between excursions Z_{1s} and Z_{2s}. $\rho(\tau)$ is the normalized form of the autocorrelation function defined by

$$R(\tau) = \lim_{L\to\infty} \frac{1}{2L}\int_{-L}^{L} Z(X)Z(X+\tau)dX, \qquad (3)$$

where X is parallel to the mean surface plane and $-Z$ is the distance below the mean surface. By definition the variance of the height distribution is

$$R(0) = \lim_{L\to\infty} \frac{1}{2L}\int_{-L}^{L} Z^2(X)dX = \sigma^2 \qquad (4)$$

and

$$\rho(\tau) = R(\tau)/R(0) = R(\tau)/\sigma^2. \qquad (5)$$

When $\tau = 0$, Z_{1s} and Z_{2s} are coincident, therefore, $\rho(0) = 1$. For $\tau = \infty$, Z_{1s} and Z_{2s} are completely uncorre-

 0021-8979/88/115346-05$02.40 © 1988 American Institute of Physics

[This article is copyrighted as indicated in the article. Reuse of AIP content is subject to the terms at: http://scitation.aip.org/termsconditions. Downloaded to] IP: 128.173.126.47 On: Wed, 06 May 2015 20:20:25

lated, and $\rho(\infty) = 0$. Between the two extremes of $\tau = 0$ and $\tau = \infty$, Z_{1s} and Z_{2s} are partially correlated with decreasing correlation for increasing τ. The function

$$\rho(\tau) = e^{-|\tau|/\tau_c} \qquad (6)$$

is commonly used in tribology and will be used in this development.[3] τ_c is a correlation distance which indicates how quickly a surface excursion loses correlation with increasing distance τ from a neighbor.

The scaled form of the conditional probability density function based upon a normal distribution is

$$p(Z_{2s}/Z_{1s},\tau) = \frac{p(Z_{1s},Z_{2s},\tau)}{p(z_{1s})} = \frac{1}{\sqrt{2\pi}\sigma[1-\rho^2(\tau)]^{1/2}} \times e^{-\{[Z_{2s}-\rho(\tau)Z_{1s}]^2/[1-\rho^2(\tau)]\}}. \qquad (7)$$

This represents the probability of an excursion Z_{2s} under the condition that a prescribed excursion Z_{1s} exists at a horizontal distance τ away.

The kinematic intensity from a polycrystalline solid is taken as a sum of intensities produced at each volume element. Consider a sample consisting of planes of signal producing elements dV (Fig. 1) located at a depth $-Z_s$ and extending to $-Z_s - dZ_s$. If the X axis is parallel to the mean surface plane, the volume element in a two-dimensional model is $dX\,dZ$. Incident ray $A' - A$ produces a signal at A which follows a signal path $A - A''$. The distance τ is measured from each element A along X. Since there are two rays that influence the detected signal, two variables, $\tau = \tau_i$ and $\tau = \tau_s$, are required, extending in $\pm$ directions from A. Two correlated conditional functions $p(Z_{is}/Z_{0s},\tau_i)$ and $p(Z_{ss}/Z_{0s},\tau_s)$ are used to describe absorption along $A' - A$ and $A - A''$ with correlation determined by $|\tau|/\tau_c$ in Eq. (6).

As shown in Fig. 1, volume elements within the same horizontal layer can be divided into groups. Each group is defined by a specific excursion height above the signal generating element and the location of the layer. For example, volume elements A,B,C,D, shown in Fig. 1, are in a common layer, and belong to the same group because the excursion heights are the same. This group is designated by (Z_s,Z_{0s}).

Clearly the strength of x-ray fluorescence or diffraction signals depends upon incident and signal ray pairs. In the present model, these are coupled relative to the intermediate signal element through $\rho(\tau)$. This approaches unity as either τ_i/τ_c or τ_s/τ_c approach zero. And, coupling increases to the extent that neighboring surface asperities must have the same z_{0s}. A large τ_c causes neighboring points along the surface to look alike. At the other extreme, a small τ_c causes nearby points to be unrelated. Here the surface asperities vary rapidly with X.

For the present, consider only the signal ray. The same development and result will be used for the incident ray. A signal ray from an element of the (Z_s,Z_{0s}) group makes an angle of θ_s with the horizontal plane (Fig. 2). Surface traces corresponding to all "elements" in this group are superimposed to illustrate the distribution of material above the signal ray. If each excursion intersects the signal ray only once, then the signal ray is completely within material below the intersection and completely outside above. The distribution of the intersections along the signal ray determines the distribution of its absorption lengths. By restricting this development to one intersection, the distribution of the intersections along the signal ray can be determined rather simply. Although a single intersection model is not valid for small θ_i and θ_s, it treats most cases normally encountered with conventional x-ray optics.

In Fig. 3, a point absorber on the signal ray is shown located at a scaled height of $Z_{ss} = Z/\sqrt{2}\sigma$ and separated by a scaled horizontal distance $\tau_s = \tau/\sqrt{2}\sigma$ from the signal generating element. Vertical lines passing through this point and the signal generating element are shown as an absorption line and a signal line. Since every excursion of the (Z_s,Z_{0s}) group crosses the absorption line once, the fraction of crossings located at or above Z_{ss} is the cumulative probability function from Z_{ss} to ∞, i.e.,

$$P(Z_{ss}/Z_{0s},\ \tau) = \sqrt{2}\sigma \int_{Z_{ss}}^{\infty} p(Z_{ss'}/Z_{0s},\ \tau_s)dZ_{ss'} = \tfrac{1}{2}\,\mathrm{erfc}\left(Z_{ss} - \rho Z_{0s}/\sqrt{1-\rho^2}\right). \qquad (8)$$

Equation (8) is valid for any point because the point absorber on the signal ray at Z_{ss} is arbitrarily chosen along the signal ray. The behavior of Eq. (8) is as expected. With ideal correlation, ρ becomes unity and erfc is either unity or zero. $P(Z_{ss} > Z_{0s}/Z_{0s},\tau) = 0$ or $P(Z_{ss} < Z_0/Z_{0s},\tau) = 1$.

Figure 3 illustrates two closely spaced absorption lines

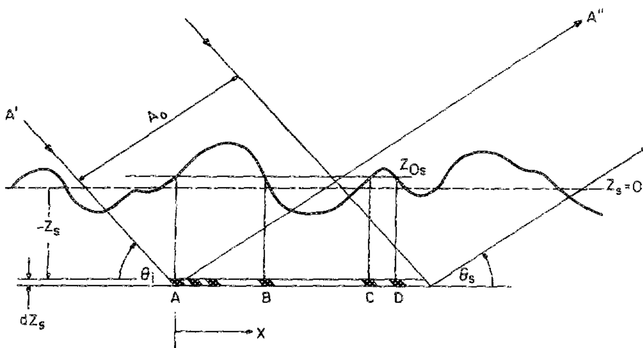

FIG. 1. A schematic diagram of extreme rays showing the signal elements and surface asperities of a like group. x-z coordinates. $\theta_i - \theta_s$ and A_0.

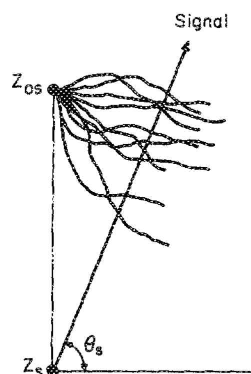

FIG. 2. Schematic diagram showing intersections with one signal ray, and surface profiles for one signal group.

[This article is copyrighted as indicated in the article. Reuse of AIP content is subject to the terms at: http://scitation.aip.org/termsconditions. Downloaded to] IP: 128.173.126.47 On: Wed, 06 May 2015 20:20:25

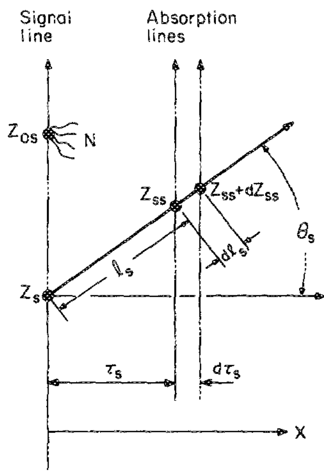

FIG. 3. Schematic diagram illustrating signal and absorption lines along with a section on the signal ray dl_s for surface profiles to cross.

intersecting the signal ray at heights of Z_{ss} and $Z_{ss}+dZ_{ss}$, respectively. If the total number of signal generating elements in the (Z_s,Z_{0s}) group is N, then the total number of excursions starting from the signal line is also N. $NP(Z_{ss}/Z_{0s},\tau_s)$ and $NP(Z_{ss}+dZ_{ss}/Z_{0s},\tau_s+d\tau_s)$ excursions are located above the signal ray at the two absorption lines, respectively. The difference

$$n=NP(Z_{ss}/Z_{0s},\tau)-NP(Z_{ss}+dZ_{ss}/Z_{0s},\tau_s+d\tau_s)$$

gives the number of excursions passing through the signal ray in the differential spacing between the two absorption lines. Because the total number of intersections between the excursions and the signal ray is also N, n out of N intersections gives an absorption length of $l_s=\sqrt{2}\sigma(Z_{ss}-Z_s)/\sin\theta_s$. Consequently, the probability density function $p(l_s)$ for the absorption length distribution becomes

$$p(l_s)dl_s=n/N=-[P(Z_{ss}+dZ_{ss}/Z_{0s},\tau_s+d\tau_s)-P(Z_{ss}/Z_{0s},\tau_s)]. \quad (9)$$

Because

$$P(Z_{ss}+dZ_{ss}/Z_{0s},\tau_s+d\tau_s)\simeq P(Z_{ss}/Z_{0s},\tau_s)+P'(Z_{ss}/Z_{0s},\tau_s)dZ_{ss},$$
$$p(l_s)dl_s=-P'(Z_{ss}/Z_{0s},\tau_s)dZ_{ss}, \quad (10)$$

the derivative of $P(Z_{ss}/Z_{0s},\tau_s)$ with respect to Z_{ss} gives the required probability density for absorption paths of length l_s but written as a function of the Z coordinate. It can be shown that

$$p(l_s)dl_s=\frac{1}{\sqrt{\pi}}\left[\exp\left(-\frac{(Z_{ss}-\rho Z_{0s})^2}{1-\rho^2}\right)\right]\times\left(\frac{1}{\sqrt{1-\rho^2}}-\frac{\rho^2Z_{ss}-\rho Z_{0s}}{\tau_{cs}\tan\theta_s(1-\rho^2)^{3/2}}\right)dZ_{ss}. \quad (11)$$

The average absorption factor for group (Z_s,Z_{0s}) is calculated from

$$\langle e^{-\mu_s l_s}\rangle=\int_0^\infty e^{-\mu_s l_s}p(l_s)dl_s=-\int_{Z_s}^\infty e^{-[\sqrt{2}\sigma\mu_s(Z_{ss}-Z_s)/\sin\theta_s]}\times P'(Z_{ss}/Z_{0s},\tau_s)dZ_{ss}, \quad (12)$$

where μ_s is the linear absorption coefficient of the sample for the signal ray.

A similar result is obtained for the incident beam by replacing θ_s with θ_i (the incident angle) and μ_s with μ_i (the linear absorption coefficient for the incident ray). With these substitutions in Eqs. (11) and (12), we obtain the average absorption attenuation factor $\langle e^{-\mu_i l_i}\rangle$ for the incident ray.

The average absorption attenuation factor for one group which includes both the incident and signal rays is taken as

$$A(Z_s,Z_{0s})=\langle e^{-(\mu_i l_i+\mu_s l_s)}\rangle=\int_0^\infty\int_0^\infty p(l_i,l_s)e^{-(\mu_i l_i+\mu_s l_s)}dl_i\,dl_s, \quad (13)$$

where l_i,l_s are related to the Z coordinate by $l_i=\sqrt{2}\sigma(Z_{is}-Z_s)/\sin\theta_i$, etc. $p(l_i,l_s)$ is the probability density for l_i and l_s, and is determined by taking the product of two functions which are correlated through the excursion height at the intermediate signal line. The mutual distribution of the intersections at the extreme ends is ignored. This approximation gives

$$A(Z_s,Z_{0s})=\langle e^{-(\mu_i l_i+\mu_s l_s)}\rangle\simeq\int_0^\infty\int_0^\infty p(l_s)p(l_i)e^{-(\mu_i l_i+\mu_s l_s)}dl_i\,dl_s=\int_0^\infty p(l_i)e^{-\mu_i l_i}dl_i\int_0^\infty p(l_s)e^{-\mu_s l_s}dl_s. \quad (14)$$

Strong pair correlation between l_i and l_s occurs when both θ_i and $\theta_s\to 90°$, while weak correlation can be associated with either θ_i or θ_s becoming small. Note that for the more common symmetrical case $\theta_i=\theta_s$ and $p(l_i)=p(l_s)$.

It is important to note that when incident and signal rays are on the same side of the sample normal, the signal line does not serve as an intermediate point. Under these conditions, mutual correlation between beam paths must also be considered. Therefore, θ_i and θ_s are restricted to a range extending from 0° to 90°.

X-RAY INTENSITY FROM THE STATISTICAL ROUGHNESS MODEL

The signal intensity contributed by a specific group (Z_s,Z_{0s}) is

$$\Delta I(Z_s,Z_{0s})=I_0Q\Delta V(Z_s,Z_{0s})A(Z_s,Z_{0s}), \quad (15)$$

where I_0 is the incident intensity. For a fluorescence signal from a specific element i,[4]

$$Q=Q_{fi}=N_i(D_i/4\pi R^2), \quad (16)$$

where $N_i=$ number of i atoms per volume, $\sigma_i=$ atomic cross section of atom i for producing fluorescence of one type, $D_i=$ dimensionless absorption factor for fluorescence

[This article is copyrighted as indicated in the article. Reuse of AIP content is subject to the terms at: http://scitation.aip.org/termsconditions. Downloaded to] IP: 128.173.126.47 On: Wed, 06 May 2015 20:20:25

radiation in the path from sample surface to detector times the detector efficiency, and $R=$ sample to detector distance. For a diffraction signal from a powder at a specific reflection,[5]

$$Q = Q_d = \text{const}\,\frac{\lambda^3}{v_c^2}\,\frac{1+\cos^2 2\theta\cos^2 2\theta'}{\sin\theta\sin 2\theta}\,jF^2, \quad (17)$$

where $Q_d=$ reflectivity, $\lambda=$ wavelength of the incident beam, $v_c=$ volume of the unit cell, $2\theta=$ Bragg angle, $2\theta'=$ Bragg angle for monochromator, $j=$ multiplicity, and $F=$ structure factor. $\Delta V(Z_s,Z_{0s})$ is the total volume of all elements in group (Z_s,Z_{0s}). Because the height distribution of excursions is normal,

$$\Delta V(Z_s,Z_{0s}) = \Delta V\sqrt{2}\sigma p(Z_{0s})dZ_{0s}, \quad (18)$$

where $p(Z_{0s})$ is the normal probability density function given in Eq. (1). Here ΔV is given by (see Fig. 1)

$$\Delta V = (\sqrt{2}\sigma A_0/\sin\theta_i)dZ_s, \quad (19)$$

where A_0 is the cross-sectional area of the incident beam. Combining Eqs. (1), (15), (18), and (19),

$$dI(Z_s,Z_{0s}) = \frac{\sqrt{2}\sigma I_0 Q A_0}{\sqrt{\pi}\sin\theta_i}\,e^{-Z_{0s}^2}A(Z_s,Z_{0s})dZ_{0s}\,dZ_s. \quad (20)$$

The intensity contributed by a layer at Z_s is simply the integral over all asperities at the signal line above Z_s:

$$dI(Z_s) = \frac{\sqrt{2}\sigma I_0 Q A_0}{\sqrt{\pi}\sin\theta_i}\int_{Z_s}^{3} e^{-Z_{0s}^2}A(Z_s,Z_{0s})dZ_{0s}\,dZ_s. \quad (21)$$

Although the upper limit should be infinity, a value of 3 causes the integrand to vanish and is readily treated in numerical calculations.

The total intensity is the summation of the intensities contributed by each layer. Integrating Eq. (21) over all possible Z_s,

$$I_{rs} = \frac{\sqrt{2}\sigma I_0 Q A_0}{\sqrt{\pi}\sin\theta_i}\int_{-\infty}^{3}\int_{Z_s}^{3} e^{-Z_{0s}^2}A(Z_s,Z_{0s})dZ_{0s}\,dZ_s. \quad (22)$$

The intensity from an ideally flat sample provides a useful reference and can be obtained by integrating the intensity scattered by each complete layer

$$I_{fs} = \int_{-\infty}^{0}\frac{I_0 Q A_0}{\sin\theta_i}\exp\left(\mu_i\frac{Z}{\sin\theta_i}+\mu_s\frac{Z}{\sin\theta s}\right)dZ$$
$$= I_0 Q A_0\frac{1}{\left[\mu_i+\dfrac{\sin\theta_i}{\sin\theta_s\mu_s}\right]}. \quad (23)$$

Again, the numerical integration of Eq. (22) is conveniently taken over ± 3 without significant truncation error. For material located below $Z_s=-3$, the surface asperities are negligible and a flat sample calculation is used:

$$\frac{I_0 Q A_0}{\sin\theta_i}\int_{-\infty}^{-3\sqrt{2}\sigma}\exp\left[\left(\frac{\mu_i}{\sin\theta_i}+\frac{\mu_s}{\sin\theta_s}\right)Z\right]dZ$$
$$= I_0 Q A_0\frac{1}{(\mu_i+(\sin\theta_i/\sin\theta_s)\mu_s)}$$
$$\times e^{-3\sqrt{2}\sigma[(\mu_i/\sin\theta_i)+(\mu_s/\sin\theta_s)]}. \quad (24)$$

This result is combined with Eq. (22) according to the previous discussion, and divided by Eq. (23). Consequently, the ratio R, giving the intensity reduction for a rough sample, is

$$R = \frac{I_{\text{rough sample}}}{I_{\text{flat sample}}} = \sqrt{2/\pi}\,\sigma\left(\frac{\mu_i}{\sin\theta_i}+\frac{\mu_s}{\sin\theta_s}\right)$$
$$\times\int_{-3}^{3}\int_{Z_s}^{3} e^{-Z_{0s}^2}A(Z_s,Z_{0s})dZ_{0s}\,dZ_s$$
$$+e^{-3\sqrt{2}\sigma[(\mu_i/\sin\theta_i)+(\mu_s/\sin\theta_s)]}. \quad (25)$$

A computer program with repeated use of 12-point Gauss-Legendre quadrature integrations is used to evaluate Eq. (25).

EXPERIMENTAL VERIFICATION OF THE STATISTICAL MODEL

The statistical model, which we have developed, is compared with measured intensities from a rough fully stabilized zirconia (FSZ), containing 8 mol % Y_2O_3, and one which is identical but is well polished. For the ground (rough) sample, we obtained $\sigma(=6.2\,\mu\text{m})$ and $\tau_c(=82\,\mu\text{m})$ by profilometer measurements. A typical surface profile for the rough sample is shown in Fig. 4, while the corresponding autocorrelation coefficient function calculated directly from the complete digitized profile, is shown in Fig. 5.

The intensity ratio given by Eq. (25) is evaluated using the σ and τ_c values of the rough sample for symmetrical diffraction and Cu$K\alpha_1$ radiation. The linear absorption coefficient for the FSZ and this radiation is 650 cm^{-1}. The calculated result is shown in Fig. 6 as the solid curve while the dashed line represents an extrapolation which is likely to be influenced by multiple surface intersections. Experimental ratios of integrated intensities measured from the flat and rough samples as shown as points in Fig. 6. These measurements were carried out using a symmetrically aligned Siemens diffractometer, and a diffracted beam quartz $K\alpha_1$ monochromator. Two overlapping slow scans (0.1°/min) were made over each peak to obtain a better statistical average. This gave a total of 12 peaks for each sample. Peak areas,

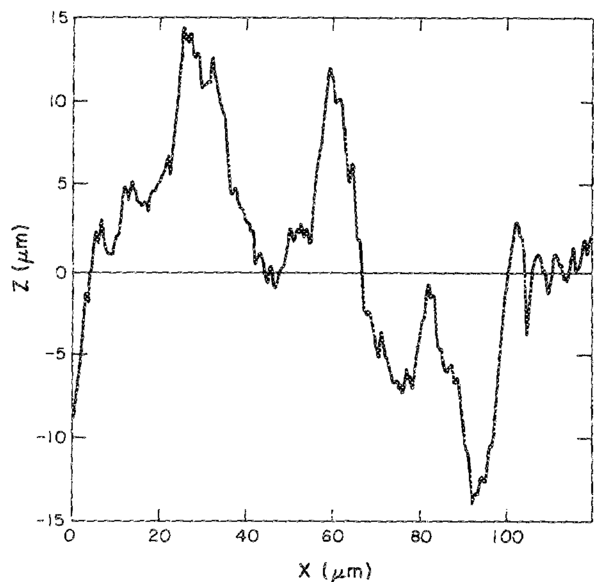

FIG. 4. Typical surface profile measurement of the ground FSZ sample.

[This article is copyrighted as indicated in the article. Reuse of AIP content is subject to the terms at: http://scitation.aip.org/termsconditions. Downloaded to] IP: 128.173.126.47 On: Wed, 06 May 2015 20:20:25

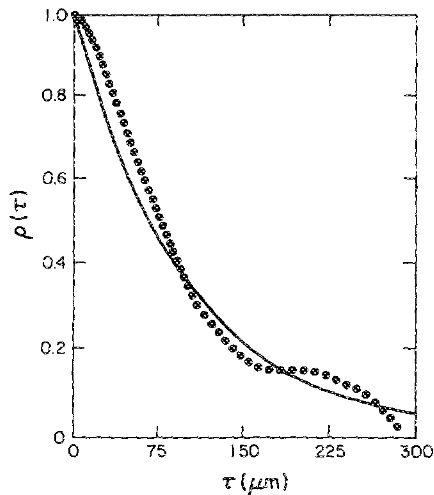

FIG. 5. Autocorrelation coefficient function for the profile shown in Fig. 4. The solid curve is used to fit indicated data points.

corrected for background, were measured using a planimeter. The theoretical calculations based on our statistical model follow the same trend as the experimental data.

DISCUSSION

An examination of the theoretical curve of Fig. 6 illustrates that no sharp minimum exists over the range of experimental observations. For a 45° sawtooth a sharp minimum is found[2] at $\theta_i = \theta_s = 45°$. Rays traveling parallel to the edge of a sawtooth experience large fluctuations in the absorption pathlengths from point to point along the X axis. It is known that these rays introduce a large correction to the intensity.[1] Changing the sawtooth angle would shift the θ position for a maximum correction. With real surfaces one finds a distribution of sawtoothlike fluctuations having nearly linear regions for either the incident beam or the signal beam to follow. When this parallel tuning between the free surface and either (or both) beam(s) occurs, the fluctuations in absorption path length produce an increase in the intensity correction. The broad intensity correction curve shown in Fig. 5 may be explained on this basis. In other words, a real surface may be treated as a distribution of slopes. If one numerically calculates the average absolute slope from the profilometer data (Fig. 1), a value of 9° is obtained. This agrees almost exactly with the minimum of Fig. 6. We point this out with a degree of caution because below this angle multiple intersections of the surface with the incident and signal rays become more likely. The theory presented here is based upon a single intersection model. If the fluctuation in path lengths is deter-

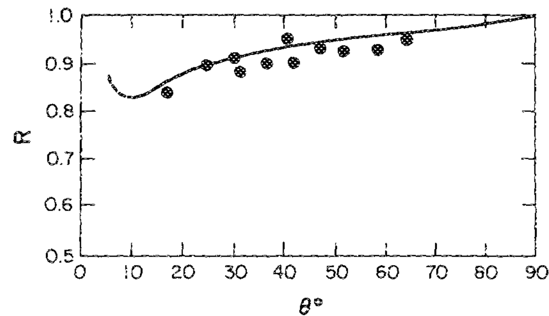

FIG. 6. Calculated (–) and experimental intensity corrections (⊗) for the ground FSZ sample.

mined largely by local fluctuations in path length near the signal element, then the minimum may be approximated by a single intersection model. A simple formula for the minimum based upon one example is given by

$$\theta_{\min} = \tan^{-1}(2.3\sigma/\tau_c). \tag{26}$$

This result is given as a rough guideline in future studies.

If one refers back to Fig. 6, one sees that as $\theta_i = \theta_s \rightarrow 90°$, the integrated intensity equals that of the ideally flat sample. This is due to complete correlation between the incident and signal rays. Also, one observes that the experimental points are systematically below the theoretical curve. This is believed to result from residual stress gradients produced in the severely ground sample.[6] Residual stresses near the surface were found to produce a range of interplanar spacings and an associated redistribution of the Bragg intensity into weak tails which are difficult to measure. A few percent of the intensity in the ground sample is lost because of this effect, causing the data points to be slightly lower than theory.

ACKNOWLEDGMENTS

This work was made available by Department of Energy Conversion and Utilization Technologies (ECUT) Program No. 19BO7733C funding. We would like to further acknowledge stimulating discussions with J. A. Carpenter of the Oak Ridge National Laboratory.

[1]R. J. Harrison and A. Paskin, Acta Crystallogr. **17**, 325 (1964).
[2]B. S. Borie, J. Appl. Cryst. **14**, 219 (1981).
[3]T. R. Thomas, *Rough Surfaces* (Longman, London, 1982), pp. 105 and 106 and 119–126.
[4]C. J. Sparks, *Synchrotron Radiation Research*, edited by H. Winick and S. Doniach (Plenum, New York, 1980), p. 459.
[5]B. E. Warren, *X-Ray Diffractions* (Addison-Wesley, Reading, PA, 1969).
[6]B. Hwang, C. R. Houska, G. E. Ice, and A. Habenschuss, **63**, 5351 (1988).

[This article is copyrighted as indicated in the article. Reuse of AIP content is subject to the terms at: http://scitation.aip.org/termsconditions. Downloaded to] IP: 128.173.126.47 On: Wed, 06 May 2015 20:20:25